Liquid Crystals
Publication details, including instructions for authors and subscription information:
http://www.informaworld.com/smpp/title~content=t713926090

Isotropic cubic phase of 4-n-pentadecyloxy-3-nitrobiphenyl4-carboxylic acid (ANBC-15): DSC, microscopic and dynamic viscoelastic studies

Shoichi Kutsumizu; Takanari Yamaguchi; Ryuji Kato; Shinichi Yano

Online publication date: 06 August 2010

To cite this Article Kutsumizu, Shoichi , Yamaguchi, Takanari , Kato, Ryuji and Yano, Shinichi(1999) 'Isotropic cubic phase of 4-n-pentadecyloxy-3-nitrobiphenyl4-carboxylic acid (ANBC-15): DSC, microscopic and dynamic viscoelastic studies', Liquid Crystals, 26: 4, 567 — 573
To link to this Article: DOI: 10.1080/026782999205010
URL: http://dx.doi.org/10.1080/026782999205010

LIQUID CRYSTALS, 1999, VOL. 26, NO. 4, 567–573

Isotropic cubic phase of 4′-*n*-pentadecyloxy-3′-nitrobiphenyl-4-carboxylic acid (ANBC-15): DSC, microscopic and dynamic viscoelastic studies

SHOICHI KUTSUMIZU*
Instrumental Analysis Center, Gifu University, 1-1 Yanagido, Gifu 501-1193, Japan

TAKANARI YAMAGUCHI
Tsukuba Research Laboratory, Sumitomo Chemical Co., Ltd., 6 Kitahara, Tsukuba, Ibaraki 300-3266, Japan

RYUJI KATO and SHINICHI YANO
Department of Chemistry, Faculty of Engineering, Gifu University, 1-1 Yanagido, Gifu 501-1193, Japan

(*Received 20 April 1998; in final form 5 November 1998; accepted 7 November 1998*)

The phase behaviour of 4′-*n*-pentadecyloxy-3′-nitrobiphenyl-4-carboxylic acid (ANBC-15) was investigated by differential scanning calorimetry, polarizing optical microscopy, and dynamic viscoelastic measurements. The phase sequence for the virgin sample of ANBC-15 is crystal–smectic C (SmC)–cubic (D)–smectic A (SmA)–'structured liquid' (I_1)–isotropic liquid (I_2) on first heating. It was found that the appearance of the D phase on the second heating depends on the top temperature of the first heating. It was also shown that the D phase is formed on heating when the preceding SmC phase is 'solid-like' from the viscoelastic point of view, i.e. storage modulus (G') > loss modulus (G'') at 62.8 rad sec^{-1}, while the 'liquid-like' SmC phase is transformed directly into the SmA phase without showing the D phase on heating. The isothermal frequency scans at a temperature in the D phase showed the existence of a cross-over point, $G' = G''$, with $G' < G''$ in the lower frequency side, suggesting a structural fluctuation of the D phase. These results are ascribed to the molecular structure of ANBC-15, which has a critical alkoxy chain length in ANBC series.

1. Introduction

Thermotropic liquid crystalline cubic phases are now attracting much research interest in the liquid crystalline field because they are optically isotropic and their structures and transformations from and to other optically anisotropic liquid crystalline phases (such as smectic phases) are not completely understood [1–3]. 4′-*n*-Alkoxy-3′-nitrobiphenyl-4-carboxylic acids, ANBC-*n*, where *n* is the number of carbon atoms in the alkoxy groups, are well known for showing one of these cubic phases when $n \geqq 15$ [4–9]. Historically, ANBC compounds were first synthesized by Gray *et al.* [4], and their phase behaviour was studied by Demus *et al.* in detail [5, 6], where the members with $n = 16$ and 18 were found to show a cubic phase called the (smectic) D phase. In 1980, Goodby and Gray found that the 3′-cyano analogues with $n = 16$ and 18 also show the D phase [7, 8], but until recently, it seemed that the appearance of the D phase was limited to these four compounds with very similar chemical structures and nearly equal molecular size. In 1994, we reinvestigated the phase behaviour of a series of ANBC-*n* to clarify how the alkoxy chain length *n* influences the appearance of the D phase, and reported that the temperature range of the D phase becomes wider, from 22 K for $n = 16$ to 57 K for $n = 22$, with increasing *n* [9].

The present study clearly shows that the alkoxy chain length plays a key role in stabilizing the D phase; ANBC-15 has a critical length of alkoxy chain, and significantly the D phase was observed from 460 to 471 K only on first heating. The phase behaviour of ANBC-15 is thus worth investigating further to elucidate other factors for stabilizing the D phase, especially in ANBC-15. In this paper, we present the results of

*Author for correspondence.

Journal of Liquid Crystals ISSN 0267-8292 print/ISSN 1366-5855 online
http://www.tandf.co.uk/JNLS/lct.htm
http://www.taylorandfrancis.com/JNLS/lct.htm

differential scanning calorimetric (DSC), microscopic, and dynamic viscoelastic studies for ANBC-15. Structural features of the D phase of ANBC-15 are discussed by comparison with the D phase of other ANBC homologues.

2. Experimental

2.1. *Preparation*

The ANBC compounds studied had $n = 15$, and 14, 16, 22 (for comparison), all of which were prepared according to the established method by Gray *et al.* [4, 10]. The samples were recrystallized from ethanol several times and confirmed to be pure by infrared (IR), ^{1}H NMR, mass spectroscopy (MS), DSC, thin layer chromatography, and elemental analysis.

2.2. *Measurements*

The IR, ^{1}H NMR, and MS spectra were recorded on a Perkin-Elmer 1640 and Perkin-Elmer system 2000 FTIR spectrometers, a JEOL JNM-α-400 spectrometer, and a Shimadzu GCMS QP-1000 system, respectively. Thermal data were collected on a Seiko Denshi DSC-210 interfaced to a TA data station (SSC 5000 system) at a heating/cooling rate of 2 or 5 K min^{-1} under a dry N_2 flow of *c.* 40 ml min^{-1}. The instrument was calibrated with indium (m.p. 156.6°C, $\Delta H = 28.458$ cal g^{-1}) and tin (m.p. 231.9°C, $\Delta H = 59.5$ cal g^{-1}). The texture of each mesophase was observed with a Nikon Optiphot-pol XTP-11 polarizing optical microscope (POM) equipped with a Mettler FP-82 hot stage at a heating/cooling rate of 2 or 5 K min^{-1}.

Viscoelastic measurements were performed by using a Rheometrics Dynamic Stress Rheometer DSR for ANBC-16 and -22 and on a Rheometrics RDS-II for ANBC-14 and -15. In both instruments, parallel plate shear geometry was employed, and the diameter of the plate and the gap between the two plates were 40.0 and 0.55 mm, respectively, in DSR, and 50.0 or 25.0 and 1.00–0.50 mm, respectively, in RDS-II. Samples were sandwiched between the two plates at a temperature above the melting point under a N_2 gas atmosphere. Two types of measurement were carried out: isochronal experiments on slow heating/cooling with a rate of 2 K min^{-1}, and isothermal frequency scans in the range 0.1–1000 rad sec^{-1}. In the former type of measurement, the strain amplitude used was in most cases 10–30% in the whole temperature region studied, to measure the resulting torque with an appropriate precision. Although much smaller strain amplitude should have been used to minimize a probable non-linear viscoelastic response [11], we confirmed that such a large strain amplitude gives no essential errors or changes in the storage and loss modulus at phase transitions for the present system; for example, a jump of the storage modulus at the transition from the smectic C (SmC) to D phase was observed, independent of the amplitude used in the range 1–30%. In the isothermal frequency scans, the strain amplitude used was 3% for the D phase temperature region, but the stress–strain hysteresis loop (Lissajous's pattern) in the D phase for ANBC-16 and -22 showed a rhombic shape owing to its non-linear response, even at a strain amplitude of less than 0.1% [12].

3. Results and discussion

3.1. *Thermal studies*

Figure 1 shows DSC heating curves for ANBC-15 with a scanning rate of 5 K min^{-1} under three types of thermal cycles. Here, only the heating curves are discussed because the cooling curves were less reproducible and

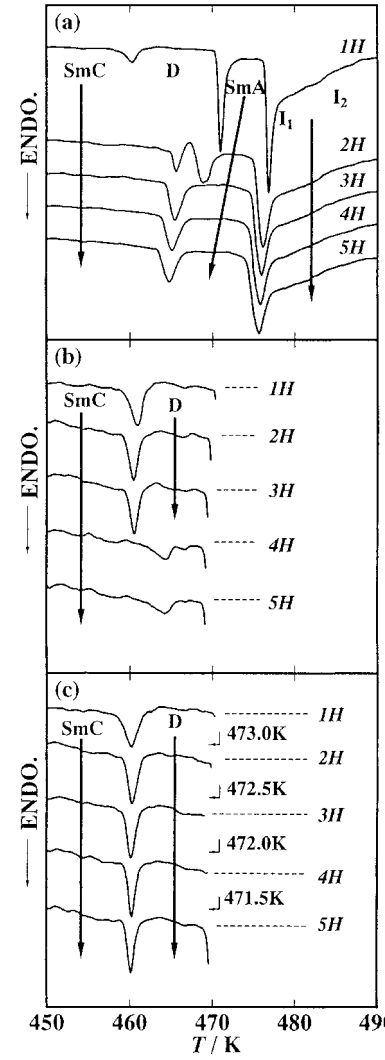

Figure 1. DSC heating curves for ANBC-15 at a rate of 5 K min^{-1}. The thermal cycles were repeated below (*a*) 498 K in the I_2 phase, (*b*) 473 K in the SmA phase, and (*c*) D–SmA phase transition temperature. In the figures, 1H, 2H, 3H, 4H, and 5H denote the first, second, third, fourth, and fifth heating scans in each thermal cycle.

seemed to be severely dependent on some unknown factor, such as nucleation and growth. The thermograms of figure 1 (*a*) apply to a top temperature of 498 K in the I_2 phase. On the first heating (denoted as 1H), ANBC-15 shows three kinds of liquid crystalline phases, the SmC (400.3–460.4 K), the D (460.4–471.0 K), and the SmA phases (471.0–476.9 K); these are characterized by a schlieren texture, a completely black area with straight edges on growing, and a strong tendency for homeotropic arrangement, respectively, when viewed by POM with crossed polarizers. Above 476.9 K, the sample appeared as isotropic liquid by POM, but the DSC curves show a broad endothermic peak (or tail) centred at ~482 K [6, 8, 9]. Like other homologues such as ANBC-16, ANBC-15 has two kinds of isotropic liquid state, I_1 (lower temperature phase) which is a structured liquid [8, 13] and the I_2 phase. The second heating (2H) behaviour was slightly complicated. When viewed by POM, the sample showed first a sand-like texture, perhaps characteristic of the SmC phase after melting. This texture was transformed to a typical schlieren texture at ~463 K, and then immediately changed to black owing to a homeotropic arrangement of the SmA phase. The DSC curve on 2H shows a pair of exothermic and endothermic peaks at 465.7 and 467.2 K, respectively, corresponding to the transient appearance of the schlieren texture mentioned above, and an endothermic peak at 468.8 K, the SmC–SmA phase transition; no D phase was visible and the SmA–I_1 transition was at 476.3 K. On the third scan and later (3H–5H), the SmC and SmA phases appeared, but both SmC–SmA and SmA–I_1 transition peaks are broader compared with the preceding scans.

When the top temperature was lowered to 473 K in the SmA phase, figure 1 (*b*), the D phase was observed repeatedly between the SmC and SmA phase temperature regions until 3H. On both 4H and 5H, a trace endothermic peak was detected around 464 K on DSC, but the POM observation showed no D phase. The onset temperature of the D–SmA (or SmC–SmA) phase transition in this cycle decreased from 470.2 K on 1H to 468.8 K on 5H, roughly a 0.4 K decrease per scan. In order to reverse the DSC scans at around the D–SmA phase transition temperature, the top temperature was lowered by 0.5 K every scan, from 473.0 K on 1H to 471.5 K on 5H in the cycle shown in figure 1 (*c*). It is easily recognized that the D phase exists until 5H; the SmC–D phase transition temperature is 460.2 ± 0.1 K, independent of scan, but the enthalpy change gradually decreases from 0.42 J mol^{-1} on 1H to 0.23 J mol^{-1} on 5H.

Figure 2 shows polarizing microphotographs near the SmC–D phase transition temperature for ANBC-15. The pictures (*a*) and (*b*) were obtained respectively, on the second cooling and third heating scans under thermal cycles below 470 K. The 'texture' of the D phase for ANBC-15 is very similar to that observed for other ANBC homologues with $n \geqq 16$ [5, 6, 9]. Completely black diamond-shaped or rectangular areas are shrinking on cooling (*a*) or growing on heating (*b*), in the SmC schlieren texture. The presence of clear boundaries is said to reflect the relatively slow destruction or growth of the D phase structure. The results illustrated in figures 1 and 2 demonstrate that the appearance of the D phase of ANBC-15 depends on the nature of the thermal cycle; if the thermal cycle is repeated below the D–SmA phase transition temperature, the D phase occurs almost reproducibly.

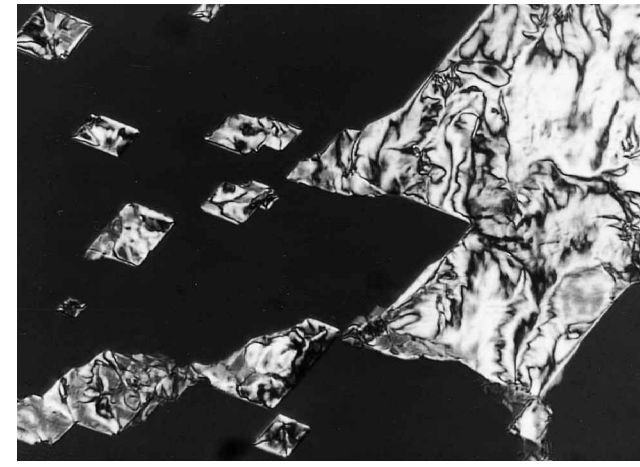

(*a*)

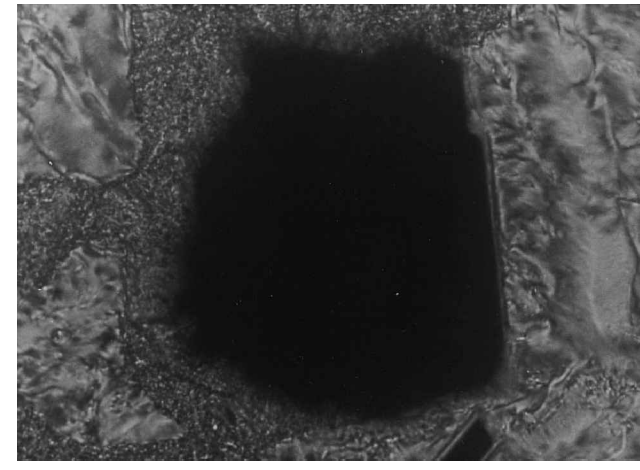

(*b*)

Figure 2. Polarizing microphotographs near the SmC–D phase transition for ANBC-15: (*a*) the second cooling and (*b*) the third heating scans under thermal cycles below 470 K.

To confirm the above conclusion, a thermal cycle was examined by DSC and POM with a scan rate of

2 K min^{-1}. The specimen of ANBC-15 was first heated to around 448 K in the SmC phase, and DSC measurement was started from the subsequent cooling process (denoted as 1C) to room temperature. The specimen was then heated to around 465 K in the D phase and cooled (on 1H and 2C, respectively). Finally, the specimen was heated to 493 K in the I_2 phase (on 2H), cooled (on 3C), and heated again to 493 K (on 3H). The results are given in figure 3, which clearly shows that the D phase appears above 459.2 K on 1H, above 451.3 K on 2C, and from 461.8 to 469.0 K on 2H, but disappears on 3C and 3H. This result is consistent with the conclusion derived from figures 1 and 2. Moreover, once heated to a temperature in the I_2 phase, the D phase was no longer observed even on heating after reversing at a temperature in the SmC phase on the preceding scan or after aging for 1 h at a mid-temperature in the SmC phase.

Furthermore, the IR and ^{1}H NMR spectra at room temperature were examined for three ANBC-15 samples with different thermal histories: a fresh sample recrystallized from the solution and not heated, and samples heated to temperatures in the D and I_2 phases. The former of the two heated samples showed the D phase but the latter not on the subsequent heating, as might have been expected from the results of figure 3. In both spectroscopic examinations no difference was observed among these three samples; also, no additional peak due to decomposition was detected for the two heated samples. This rules out the possibility that the complicated phase behaviour of ANBC-15 might simply be the result of thermal decomposition during heating.

3.2. *Viscoelastic studies*

Figure 4 shows the temperature dependence of the storage modulus (G') and loss modulus (G'') at 6.28 rad s^{-1} on a heating run at a rate of 2 K min^{-1} for (*a*) ANBC-14, (*b*) ANBC-16, and (*c*) ANBC-22. (The data for ANBC-16 and -22 were published elsewhere [12], but are cited here to aid comparison.) ANBC-16 and -22 undergo a transition from the SmC to the D phase at 449 and 412 K, respectively, on heating; as shown in (*b*) and (*c*), respectively, the dynamic viscoelastic properties of these two compounds show an abrupt change at the transition. The G' value, which is 10^3–10^4 dyn cm^{-2} in the SmC phase, jumps at the transition temperature and reaches 10^7 dyn cm^{-2} in the D phase temperature region. The G'' value changes in a similar way, but the difference between G' and G'' in the D phase becomes larger; G' is 2–4 times larger than G'' in the SmC phase while about

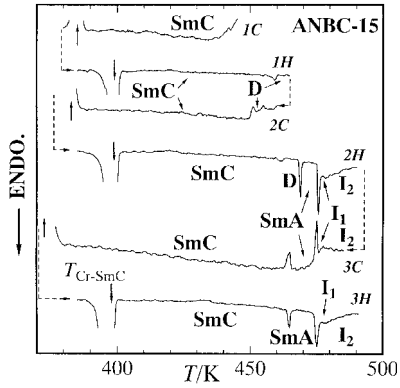

Figure 3. DSC curves of ANBC-15 at a heating/cooling rate of 2 K min^{-1}. The thermal cycles used are described in the text.

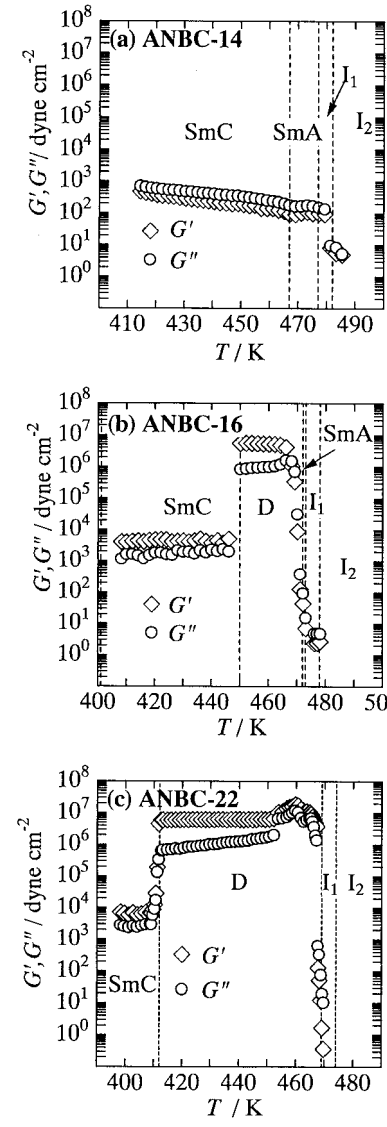

Figure 4. Temperature dependence of the storage modulus (G') and loss modulus (G'') at 6.28 rad s^{-1}, heating rate 2 K min^{-1}, for (*a*) ANBC-14, (*b*) ANBC-16, (*c*) ANBC-22; (*b*) and (*c*) reprinted from *Chem. Phys. Lett.*, **240,** Yamaguchi, T., Yamada, M., Kutsumizu, S., and Yano, S., 105, Copyright (1995), with permission from Elsevier Science.

one order of magnitude larger in the D phase (except at the high temperature side of this phase). These results indicate that the D phase is much stiffer than the SmC phase. The large resistivity against shear distortion allows us to conclude that the Tardieu and Billard interpenetrating jointed (IPJR) model [14] is appropriate for the D phase, because the three-dimensional network structure constructed by rod-like micelles could largely resist against the shear distortion. On the other hand, for ANBC-14, the values of G' and G'' lie in the order of 10^2–10^3 dyn cm^{-2} in the SmC and SmA phases, with G' 30–40% less than G''. This result is in contrast with those for ANBC-16 and -22 since ANBC-16 and -22 show $G' > G''$ in the SmC phase while $G' < G''$ in the SmC phase of ANBC-14. From the viscoelastic point of view, the structure of SmC phase of ANBC-14 is more liquid-like than those of ANBC-16 and -22. Since ANBC-16 and -22 show the D phase and ANBC-14 does not, it is suggested that the structural state of the SmC phase is connected with whether the D phase appears in the higher temperature side. This suggestion is confirmed by the next experiment for ANBC-15.

Figure 5 shows the temperature dependence of G' and G'' for ANBC-15 at an angular frequency of 62.8 rad s^{-1} at a heating/cooling rate of 2 K min^{-1}. The thermal cycle used was the same as in the DSC measurements in figure 3. The first thing to note is that in the D phase, which was observed on the first heating (1H), second cooling (2C), and second heating (2H), the G' value is 10^4–10^6 dyn cm^{-2}, larger than the value obtained for the SmC phase of the same compound. This enhancement in G' is the same phenomenon as observed for the D phase of ANBC-16 and -22, see figures 4(*b*) and 4(*c*). However, the magnitude itself is one or two orders smaller than the changes in ANBC-16 and -22. One reason proposed for this is that the D phase of ANBC-15

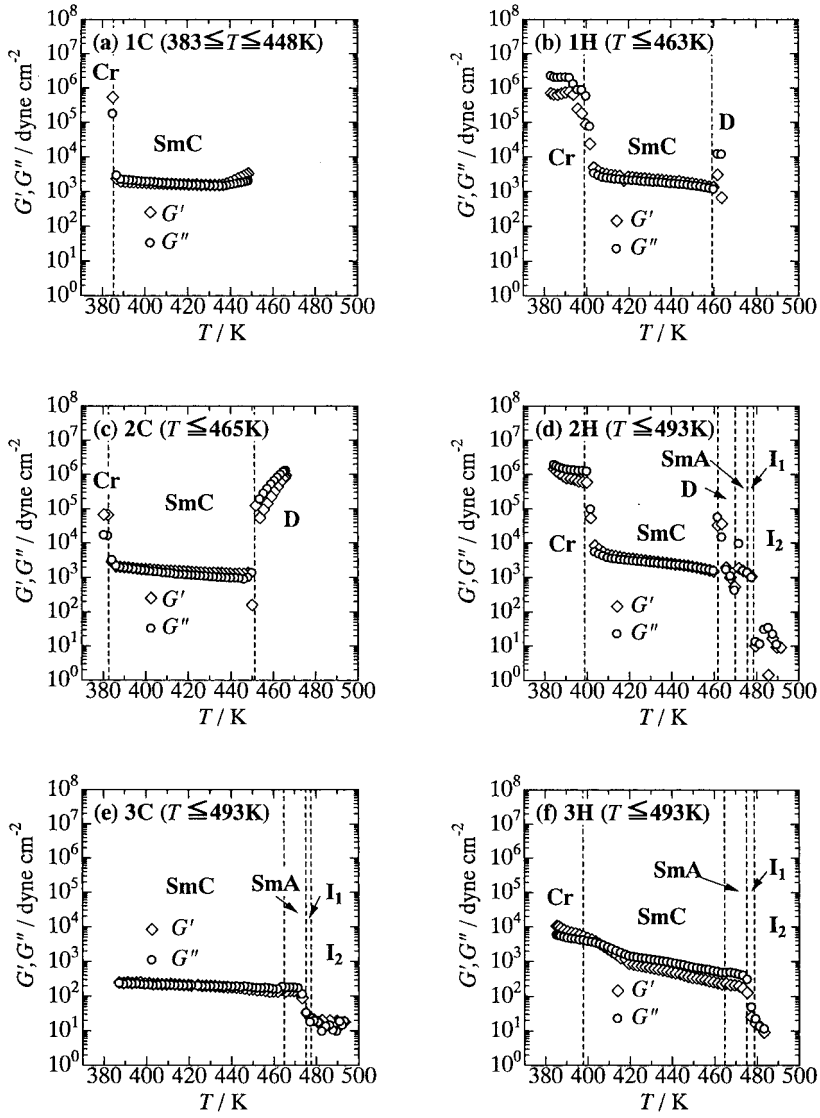

Figure 5. Temperature dependence of G' and G'' for ANBC-15 at an angular frequency of 62.8 rad s^{-1} at a heating/cooling rate of 2 K min^{-1}. The thermal cycles used are the same as for figure 3.

is essentially less stable than in ANBC-16 or -22. Another possible reason comes from the experimental conditions used, especially on 1H; the temperature was raised to 465 K just above the SmC–D phase transition temperature on 1H and after that, to start the 2C scan, decreased so quickly that the D phase had insufficient time to stabilize. In fact, the initial value of G' in the D phase region on 2C is larger than the final value on 1H.

It should also be mentioned that the reproducibility on 2H, especially in the D phase temperature region, was poorer than on other scans. Figure 6 shows a comparison of three-fold experiments for the 2H scan. All the experiments show the enhancement in G' in the D phase temperature region, but its value ranges between 10^5 and 10^7 dyn cm^{-2}. This scattering, which is large compared with that in the SmC phase region on 2H, is also ascribed to the instability of the D phase of ANBC-15. The instability that the D phase of ANBC-15 shows will be discussed later in more detail.

The second point to note from figure 5 is that, in the SmC phase, the G' value on the third cooling (3C) and heating (3H) processes is one order of magnitude smaller than the value from 1C to 2H. This difference shows that the SmC phase on both 3C and 3H is more liquid-like than the same phase of 1C to 2H. This result encourages us to conclude that the structural state of the SmC phase is related to whether the D phase appears in the higher temperature side.

Figure 7 shows isothermal frequency scans at several temperatures for (*a*) ANBC-15, (*b*) ANBC-16, and (*c*) ANBC-22. For ANBC-22, all the selected temperatures belong to the D phase region†, where G' and G'' are independent of frequency in the range 10^{-1}–10^2 rad s^{-1}. Here $G' > G''$, reflecting a solid-like response to the applied stress in the D phase, but the difference between G' and G'' is gradually decreased as the temperature approaches the D–I_1 phase transition temperature. For ANBC-16, $G' > G''$ at 408 and 438 K in the SmC phase as well as at 458 K in the D phase. In the D phase of

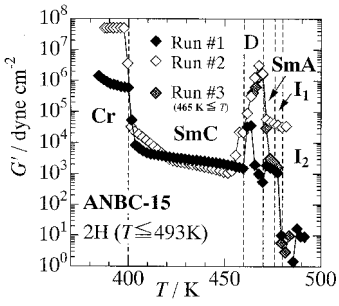

Figure 6. Comparison of three-fold experiments for the 2H scan for ANBC-15.

†A small discrepancy of a few K exists between the DSC and viscoelastic data, see also figure 4 (*c*).

ANBC-16, however, the G' and G'' are dependent on frequency below 10 rad s^{-1}, unlike in the D phase of ANBC-22; the difference between G' and G'' tends towards zero with reducing frequency. Of greater interest is the frequency dependence of G' and G'' for ANBC-15, the data being collected during the 2C process in the same thermal cycles as in figures 3 and 5. First, two isothermal scans measured at the D phase temperatures contain a cross-over point where $G' = G''$; the cross-over frequency (ω_C) is $(3\text{–}4) \times 10^1$ rad s^{-1}, below which $G' < G''$ is obtained. Second, at 423 and 443 K in the SmC phase $G' \leqslant G''$ in the frequency range 1–10^3 rad s^{-1}. The second observation indicates that the viscoelasticity of the SmC phase in ANBC-15 is liquid-like, similar to the SmC phase of ANBC-14, figure 4 (*a*), but in contrast with the SmC phase of ANBC-16, figure 7 (*b*). This is interesting, considering that ANBC-16 shows an enantiotropic and stable D phase while ANBC-14 does not; and that ANBC-15 is situated in between the other two ANBC compounds and the appearence of the D phase is largely dependent on the thermal cycle. It is concluded that in the ANBC series the structure of the SmC phase that exists at the lower temperature side of the D phase (even if only partly) can influence the appearance of the D phase. Of course, this aspect of D phase formation should be examined further, and X-ray diffraction studies are now in progress in our laboratories.

Regarding the $G' = G''$ cross-over point, this indicates another interesting aspect of the D phase of ANBC-15, i.e. an instability or a fluctuation. The existence of the ω_C means that when the frequency of the applied stress is larger than ω_C the cubic structure acts as a 'solid', while it acts as a 'liquid' at frequencies lower than ω_C. Thus, the cubic structure of ANBC-15 fluctuates in the time scale characterized by the ω_C. This interpretation is also supported by the fact that the G''-frequency curve shows a relaxational peak near ω_C. A similar observation was reported by Bates and co-worker on the phase behaviour of a series of poly(ethylene)-poly(ethylethylene) diblock copolymers [15]. They found that two cubic phases, a body-centred cubic lattice consisting of spheres with $Im3m$ symmetry and a bicontinuous structure of space group $Ia3d$, have a cross-over point of G' and G'' with $G' < G''$ on the lower frequency side of their isothermal frequency scans; they ascribed the regime $G' < G''$ to a fluctuation associated with a local disruption of 3-dimensional order existing in the cubic phases. In polymeric materials, a non-equilibrium nature or structural fluctuation of the system is frequently and relatively easily observed but, to our best knowledge, the finding in ANBC-15 is the first example from low molecular mass liquid crystalline systems. It should be also emphasized that the existence of the cross-over frequency in the D phase is closely related to a molecular structural

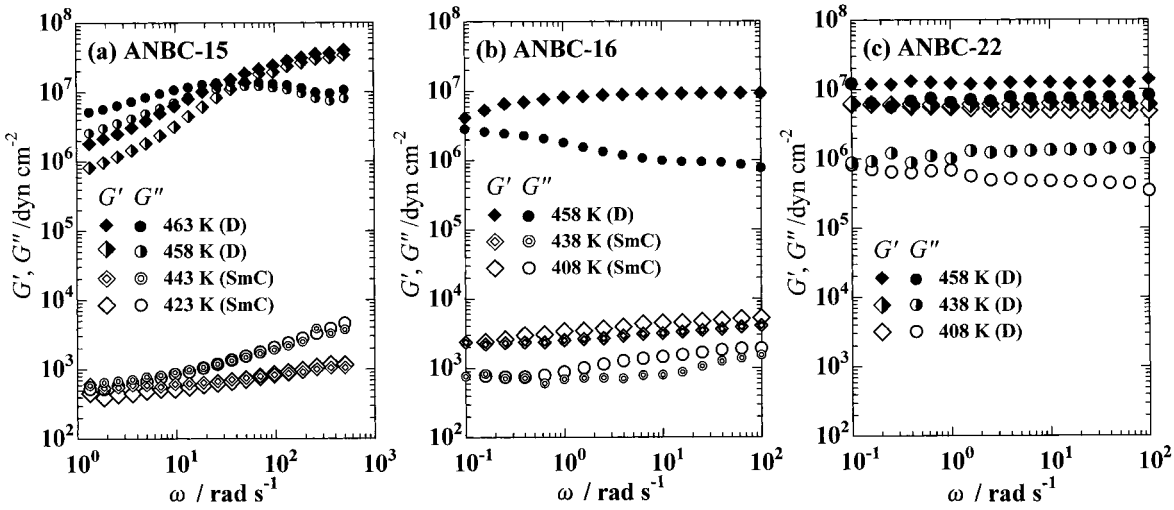

Figure 7. Isothermal frequency scans at several temperatures for (*a*) ANBC-15, (*b*) ANBC-16, (*c*) ANBC-22.

feature of ANBC-15 which has a critical alkoxy chain length for the appearance of the D phase in the ANBC series.

This study has demonstrated that viscoelastic measurements are very useful in the investigation of the dynamic properties of liquid crystal phases.

4. Conclusion

In the present study, we have determined the phase behaviour of ANBC-15 by use of a combination of DSC, POM, and dynamic viscoelastic measurements. The phase sequence for the virgin sample is crystal–SmC–D–SmA-'structured liquid' (I_1)–isotropic liquid (I_2) on first heating. The sequence on the second heating is dependent on the top temperature of the first heating. When the top temperature is below the D–SmA transition temperature, ANBC-15 shows the D phase on subsequent heating; however, having heated to a temperature in the I_2 phase the SmC phase becomes more liquid-like, and on subsequent heating is transformed directly to the SmA phase without showing the D phase. Viscoelastic measurements revealed the existence of a cross-over point of G' and G'' with $G' < G''$ on the lower frequency side in the isothermal frequency scans in the D phase. This result indicates a structural fluctuation of the D phase, closely related to the molecular structure of ANBC-15, which has a critical alkoxy chain length in the ANBC series.

We thank Mr Minoru Yamada (now at NTT) and Mr Tatsuya Ichikawa of Gifu University for their kind help. Thanks are also due to Ms Yumiko Murase and Miyuki Kasuga of the Instrumental Analysis Center, Gifu University, for the measurement of MS spectra; also to Elsevier Science for permission to reproduce in modified form figure 1 cited in ref. [12]. We are also grateful for fruitful discussions with Prof. Keiichi Moriya of the Faculty of Engineering, Gifu University.

References

[1] Demus, D., 1994, in *Liquid Crystals*, Vol. 3, edited by H. Stegemeyer, Topics in Physical Chemistry (New York: Springer), pp. 1–50.

[2] Gray, G. W., and Goodby, J. W., 1984, *Smectic Liquid Crystals: Textures and Structures* (Leonard Hill).

[3] Pershan, P. S., 1988, *Structure of Liquid Crystal Phases* (World Scientific).

[4] Gray, G. W., Jones, B., and Marson, F., 1957, *J. chem. Soc.*, 393.

[5] Demus, D., Kunicke, G., Neelsen, J., and Sackmann, H., 1968, *Z. Naturforsch.*, **23a,** 84.

[6] Demus, D., Marzotko, D., Sharma, N. K., Wiegeleben, A., 1980, *Krist. Tech.*, **15,** 331.

[7] pp. 68–81 in [2], including earlier references on cubic phases.

[8] Gray, G. W., 1986, in Zehn Arbeiten Uber Flüssige Kristalle, Kongress-und Tagung-berichte der Martin-Luther-Universität, Halle-Wittenberg, pp. 22–42.

[9] Kutsumizu, S., Yamada, M., and Yano, S., 1994, *Liq. Cryst.*, **16,** 1109; the purity of ANBC-22 was somewhat increased and the transition temperatures reported in this original paper revised on the basis of DSC (5 K min^{-1}) as crystal–375 K–SmC–412 K–D–469 K–I_1–474 K–I_2 in [13].

[10] Gray, G. W., Hartley, J. B., and Jones, B., 1955, *J. chem. Soc.*, 1412.

[11] Asada, T., Maruhashi, Y., and Onogi, S., 1975, *J. Phys. Coll.*, **36,** C1-299.

[12] Yamaguchi, T., Yamada, M., Kutsumizu, S., and Yano, S., 1995, *Chem. Phys. Lett.*, **240,** 105.

[13] Kutsumizu, S., Kato, R., Yamada, M., and Yano, S., 1997, *J. phys. Chem. B*, **101,** 10 666.

[14] Tardieu, A., and Billard, J., 1976, *J. Phys. Coll.*, **37,** C3-79.

[15] Zhao, J., Majumdar, B., Schulz, M. F., Bates, F. S., Almdal, K., Mortensen, K., Hajduk, D. A., and Gruner, S. M., 1996, *Macromolecules*, **29,** 1204.